Structure Characterization of Films from Drying Oils Cured Under Infrared Light

Yi Wang, Graciela W. Padua

Department of Food Science and Human Nutrition, University of Illinois at Urbana-Champaign, Urbana, Illinois 61801

Received 13 April 2009; accepted 2 August 2009
DOI 10.1002/app.31260
Published online 15 October 2009 in Wiley InterScience (www.interscience.wiley.com).

ABSTRACT: Drying oils have been considered as water resistant coatings for bio-based packaging materials; however, their curing rates are slow for industrial applications. Infrared radiation was investigated in this study as a means to increase the curing rate of linseed and tung oils. The effect of oil pretreatment with gamma radiation was also investigated. FTIR spectroscopy was used to monitor chemical changes during oil oxidation. Results indicated that infrared radiation increased the curing rate of linseed and tung oils. The oxidation rate of both oils, as monitored by the decrease of the 3010 cm^{-1} FTIR peak, followed an exponential decay. The structure of cured films was examined by SEM. Images of films cross section were used to develop a qualitative model of the curing process. Linseed and tung oil showed differences in structural development during drying. In the case of linseed oil, the formation of a tough skin layer slowed down oxygen diffusion to the oil underneath, resulting in slow curing. For the case of tung oil, the skin layer shrank as it formed allowing oxygen diffusion and fast curing of tung oil. © 2009 Wiley Periodicals, Inc. J Appl Polym Sci 115: 2565–2572, 2010

Key words: biobased; linseed oil; tung oil; oil oxidation; curing of drying oils; infrared assisted drying; FTIR monitoring of oil oxidation; structure of drying oil films

INTRODUCTION

Bio-based materials are being investigated for their potential as sustainable food packaging alternatives. However, many presently available products are markedly hydrophilic, and humid environments adversely affect their dimensional stability and barrier properties.[1]

Drying oils are being considered as bio-based water resistant coatings for their ability to cure or polymerize in air and form hydrophobic films. Drying oils form tough, solid, and transparent or semi-transparent films. They can be applied to the surface of conventional bio-based materials to improve their water resistance. Drying oils have been used as varnish in industrial and artistic applications since ancient times.[2–7] Examples of drying oils are linseed oil and tung oil. Linseed oil forms smooth solid films with good mechanical and water barrier properties.[2,8–10] Tung oil is used as drying agent for paints.

Drying oils contain unsaturated fatty acids, normally C_{18} with 1, 2, or 3 double bonds, and saturated fatty acids of C_{12}, C_{14}, C_{16}, and C_{18}.[8,11] Linseed oil contains 48% linolenic acid (18 : 3), 22% oleic acid (18 : 1), 16% linoleic acid (18 : 2), and 10% saturated fatty acids. Tung oil is made of 80% 9,11,13-octadecatrienoic acid with conjugated double bonds,[8,12–15] 8% oleic acid (18 : 1), 5% saturated fatty acids, 4% linoleic acid (18 : 2), and 3% linolenic acid (18 : 3). Oil drying is an autoxidation reaction that uses atmospheric oxygen. Fatty acids are oxidized, cleaved, and crosslinked with each other to build large polymers of high molecular weight.

Oil drying or curing is a very slow process that limits its applications in industry. Metallic catalysts or driers are commonly used to speed up polymerization.[4,16–19] However, metal catalysts are often toxic and food related applications of drying oils are in need of alternative methods to increase their curing rate. Because oil oxidation reactions are accelerated by light, radiation of several wavelengths has been investigated to increase the curing rate of drying oils. Mosiewicki et al.[20] reported that UV accelerated the curing of linseed oil resin/styrene thermosets. Because of its capability to induce free radical formation,[21–23] gamma radiation was investigated in previous work[12] as an agent to promote oil curing. Oil pretreatment at 50 kGy was found to increase drying rate of linseed and tung oils.[12]

The objectives of this study were to investigate the effect of infrared radiation on the rate of oxidation of linseed and tung oils and to examine the

Correspondence to: G. W. Padua (gwpadua@illinois.edu).
Contract grant sponsor: U.S. Department of Energy, (Center for Microanalysis of Materials, University of Illinois); contract grant number: DEFG02-91-ER45439.

microstructure of polymerized films. Fourier transform infrared spectroscopy (FTIR) was used to monitor chemical changes upon oil drying. FTIR had been used in previous studies to investigate the oxidation of drying oils.[3,8,12,19,20,24,25,26] A peak centered around 3010 cm^{-1} corresponding to =C—H vibration in *cis* alkenes was found useful to monitor oil oxidation. Film morphology was examined by scanning electron microscopy (SEM).

MATERIALS AND METHODS

Materials

Linseed oil and tung oil were from Sigma–Aldrich (St. Louis, MO). Acetone was ACS Spectroscopic grade, ≥99.5% (Sigma–Aldrich, St. Louis, MO).

Irradiation treatment

Linseed and tung oils were mixed with acetone at ratios of 0%, 25%, and 50% acetone (v/v) and placed in 30 mL bottles (Fisher Scientific, Pittsburgh, PA). Oil and acetone mixtures were irradiated in a lab size irradiator (Gamma Cell 2000, MDS Nordion, Canada) loaded with a cobalt-60 source. The irradiation dose applied was 0, 25, or 50 kGy. After irradiation, samples were kept in the dark, under refrigeration until curing.

Infrared drying

A medium wave curing lamp, 1500W (Caswell, Lyons, NY), was used as an infrared source to cure drying oil samples. Samples, either for SEM or FTIR, were placed at 30 cm distance under a 36″ long infrared lamp to receive uniform power. An infrared gun thermometer (Fisher Scientific, Pittsburgh, PA) was used to measure the surface temperature of oil samples during drying. The temperature was kept between 110 and 115°C.

FTIR measurements

Samples for FTIR were prepared by placing 50 μL oil drops on polyethylene sample cards (International Crystal Labs, Garfield, NJ). Sample cards were allowed to cure either under infrared light or at room conditions. FTIR spectra were collected (resolution 2 cm^{-1}, 64-scan summation) using a Thermo Nicolet FTIR spectrometer (Nexus 670, Madison, WI). Spectra were collected at 5–10 min intervals for 2 h during the drying process of infrared cured samples and at 0, 2, 6, 9, 13, and 24 h for samples cured at room conditions (no infrared light).

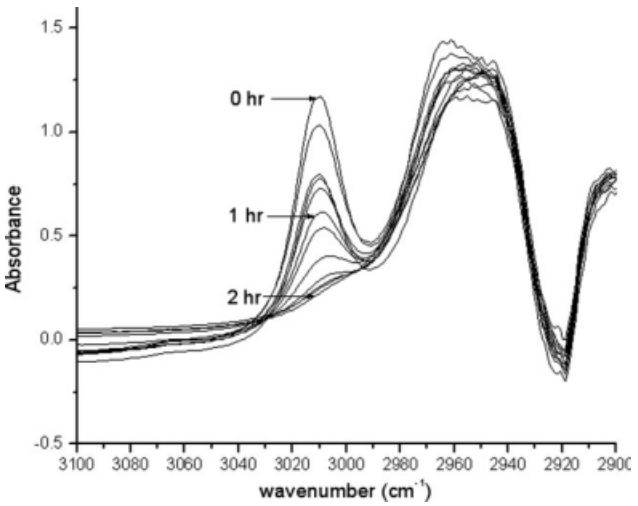

Figure 1 FTIR spectra of linseed oil cured under infrared light. Spectra were collected at 5–10 min intervals for 2 h.

Scanning electron microscopy

Samples for SEM were prepared by placing 50 μL oil drops on 20 mm × 40 mm glass slides of 150 μm in thickness. Samples were 100–200 μm in thickness and allowed to cure either under infrared light or at room conditions. Before SEM, samples were freeze fractured using liquid nitrogen. Sample cross sections were coated with gold (300 Å) to increase conductivity, using an Edwards S 150 B sputter coater. The sample cross sections were imaged with a SEM (JEOL 6060LV, Tokyo, Japan). The SEM was operated at an accelerating voltage of 20 kV at a working distance of 8–20 mm.

RESULTS AND DISCUSSION

Effect of infrared radiation on drying rate

FTIR was used to detect chemical changes during autoxidation of linseed and tung oils. Figure 1 shows a typical spectra of linseed oil dried under infrared light. Peaks observed at about 3010 cm^{-1} were attributed to the olefinic (=C—H) stretching vibration arising from fatty acid unsaturation.[3,8,25,26] *Cis* =C—H bond absorption was observed at 3010.57 cm^{-1} in linseed oil, at 3007.5 cm^{-1} in rapeseed oil, and at 3005.4 cm^{-1} in olive oil.[27] Linseed oil showed a peak at 3010.5, which gradually shifted to 3010.26 cm^{-1}. It was attributed to the migration and reconfiguration of *cis* =C—H bonds to *trans* =C—H bonds.[17] The peak decreased to a flat line after 2 h of drying, suggesting a relatively rapid depletion of *cis* =C—H bonds by a fast pace oxidation process. Figure 2 shows the FTIR spectra of the same oil dried at room conditions (not assisted by infrared light). In the latter case, the 3010 cm^{-1} peak

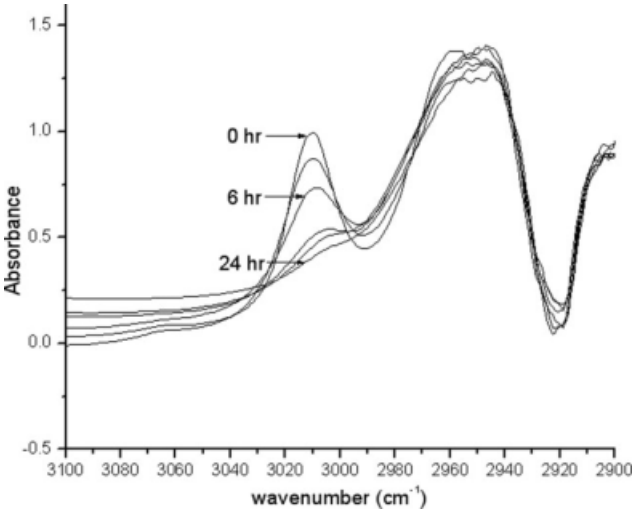

Figure 2 FTIR spectra of linseed oil cured at room conditions (not assisted by infrared light). Spectra were collected at 0, 2, 6, 9, 13, and 24 h.

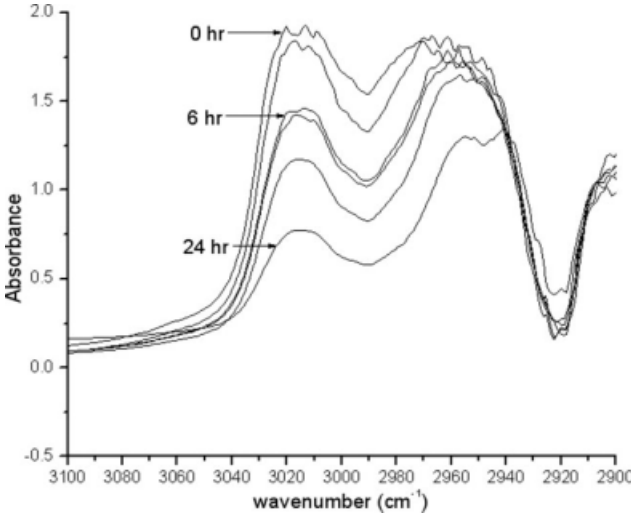

Figure 4 FTIR spectra of tung oil cured at room conditions (not under infrared light). Spectra were collected at 0, 2, 6, 9, 13, and 24 h.

decreased to the same level as in Figure 1 only after 24 h of drying, suggesting a slower oxidation process relatively to samples dried under infrared light.

Figures 3 and 4 show typical spectra of tung oil samples dried under infrared light and dried at room conditions (not assisted by infrared light), respectively. For tung oil, the *cis* =C—H stretching peak was at 3015.3 cm^{-1} and gradually shifted to 3013.6 cm^{-1}. Figure 3 shows a rapid decrease of the 3015.3 cm^{-1} peak for the sample cured under infrared light. In Figure 4, the peak decreased slowly and reached the same level as in Figure 3 only after 24 h of drying. This suggested, as in the earlier case, a slower oxidation process relatively to samples dried under infrared light.

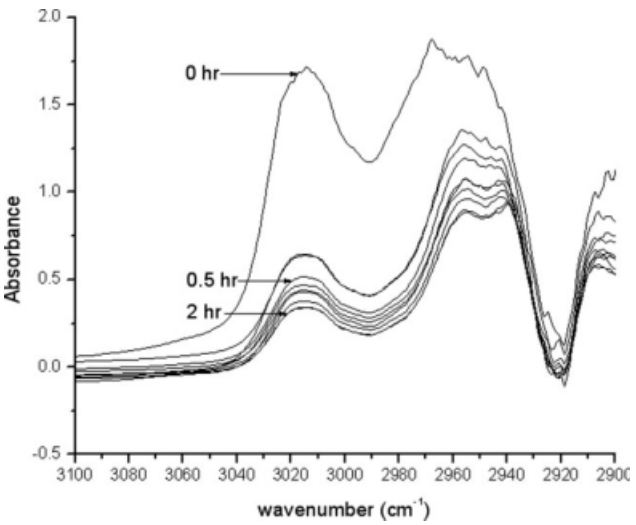

Figure 3 FTIR spectra of tung oil cured under infrared light. Spectra were collected at 5–10 min intervals for 2 h.

Effect of gamma radiation on drying rate

The drying rate of both linseed and tung oils also increased with the gamma radiation dose of oil pretreatment. Figure 5 shows the decrease of the 3010 cm^{-1} peak for linseed oil pretreated with gamma radiation and cured under infrared light. Curves were fitted with exponential decay functions: $Abs = Abs_0 * \exp(-t/k)$, where Abs_0 was the initial absorbance and $1/k$ was the rate constant of peak decay. Values of k for radiation levels of 0, 25, and 50 kGy were 20.24 ($R^2 = 0.98$), 18.11 ($R^2 = 0.99$), and 5.16 ($R^2 = 0.99$), respectively. k values indicated that the curing rate increased with radiation dose for linseed oil. The high R^2 values indicated a good curve fitting for each radiation dose. Gamma irradiation may have helped to produce free radicals in the linseed oil samples, which in turn increased the rate of oil polymerization. Results are consistent with previous work in our lab[12] where the 3010 cm^{-1} FTIR peak was used to monitor the oxidation of pretreated linseed oil cured at room conditions. The 3010 cm^{-1} peak also decreased with time following an exponential function in a similar way as described earlier.

Figure 6 shows the decrease with time of the 3015 cm^{-1} peak for tung oil pretreated with gamma radiation and cured under infrared light. Curves were fitted as earlier, yielding k values of 19.89 ($R^2 = 0.96$), 13.58 ($R^2 = 0.99$), and 6.92 ($R^2 = 0.99$) for radiation dose levels of 0, 25, and 50 kGy, respectively. For tung oil, k values also indicated that the rate of curing increased with gamma radiation dose. Gamma radiation dose had a similar effect on tung oil cured at room conditions (not under infrared light). Figure 7 shows the 3015 cm^{-1} peak decreasing with time during the oxidation process. Curves were

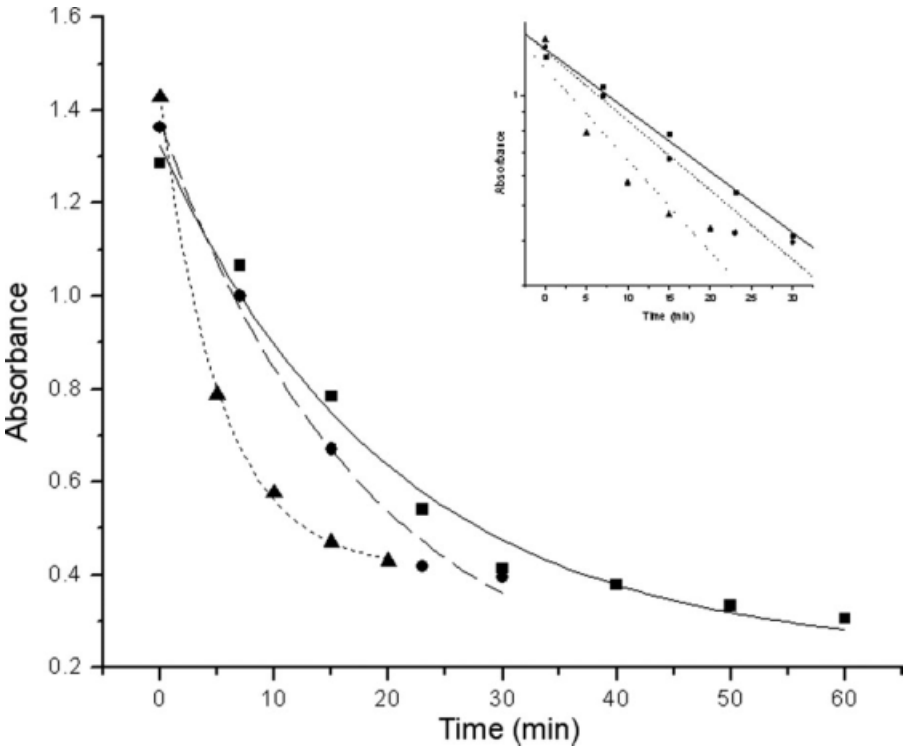

Figure 5 Effect of gamma radiation dose on 3010 cm^{-1} absorbance of linseed oil cured under infrared light: (■) 0 kGy, (●) 25 kGy, and (▲) 50 kGy. Lines represent fitted exponential functions for each radiation level. (Inset) Semilog plot of the initial part of each curve.

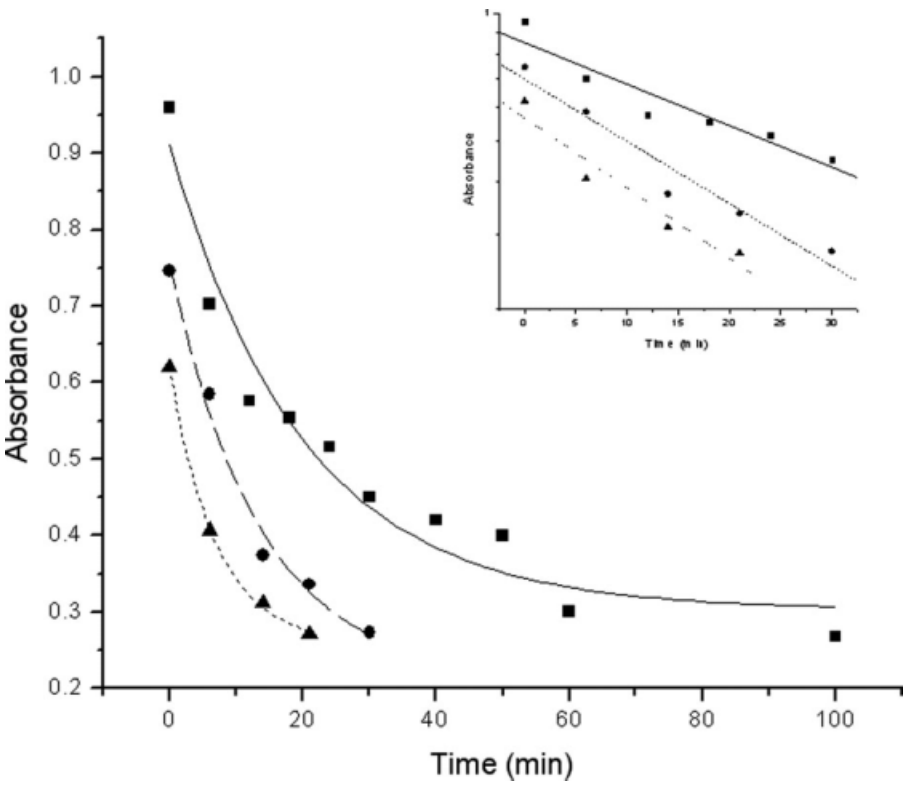

Figure 6 Effect of gamma radiation dose on 3015 cm^{-1} absorbance of tung oil cured under infrared light: (■) 0 kGy, (●) 25 kGy, and (▲) 50 kGy. Lines represent fitted exponential functions for each radiation level. (Inset) Semilog plot of the initial part of each curve.

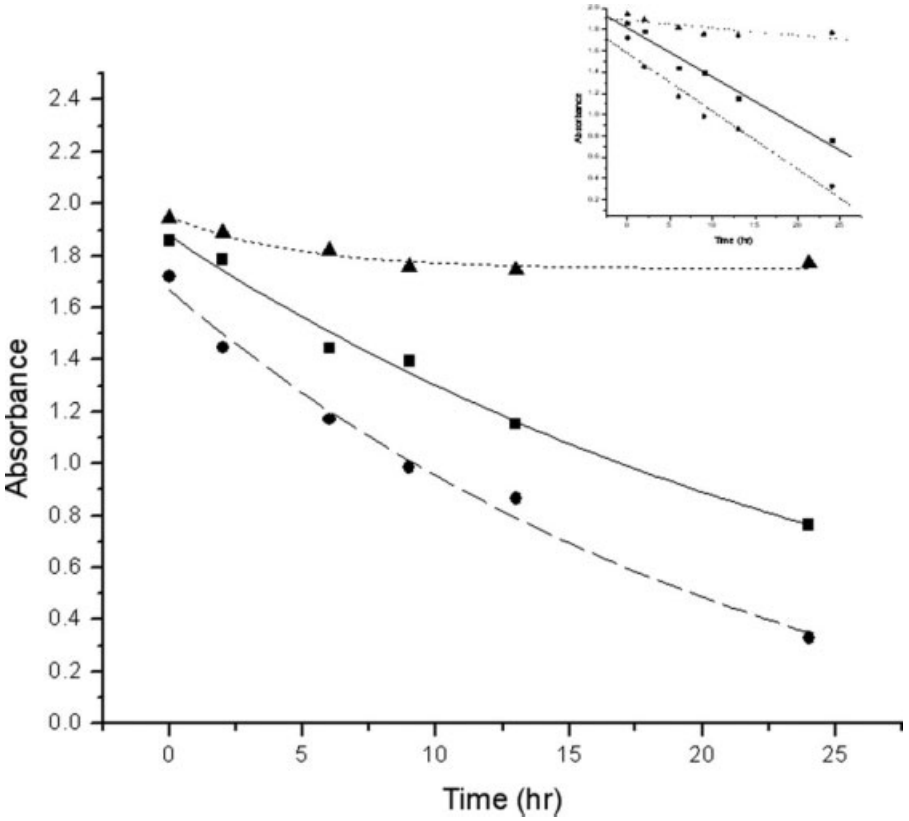

Figure 7 Effect of gamma radiation dose on 3015 cm^{-1} absorbance of tung oil cured at room conditions (not under infrared light): (■) 0 kGy, (●) 25 kGy, and (▲) 50 kGy. Lines represent fitted exponential functions for each radiation level. (Inset) Semilog plot of the initial part of each curve.

fitted as earlier and values of k were 28.81 (R^2 = 0.99), 23.10 (R^2 = 0.98), and 4.56 (R^2 = 0.95) indicating a similar trend. In summary, the oxidation rate of both tung and linseed oils followed an exponential decay model, indicating a first-order reaction kinetics with respect to the decrease in *cis* alkene bonds. Oil pretreatment with gamma radiation increased the drying rate of linseed and tung oils irrespective of exposure to infrared light during drying. The location of the *cis* =C—H stretching peak in the FTIR spectra of linseed or tung oils was not affected by pretreatment with gamma radiation.

Structure characterization of cured films

SEM images in Figures 8 and 9 show the morphology of linseed oil films cured on glass slides. Samples in Figures 8 and 9 were pretreated with gamma radiation at 0 and 25 kGy, respectively, and dried under infrared light for 10 h. Images were taken from the freeze-fracture surfaces of films. In general, films appeared to be formed by layers. The top layer, showing similar morphology in both images, had a smooth and uniform surface, which was associated with brittle fracture. In contrast, the bottom layers show a rough morphology, corresponding with ductile failure.

SEM images may reveal ductile and brittle characteristics of materials by showing texture patterns on the fracture surface. Generally, smooth surfaces indicate a brittle fracture, whereas roughness implies ductile failure. Lin et al.[28] investigated blends of polylactide and poly(ester amide). SEM images showed changes from brittle to ductile fractures.

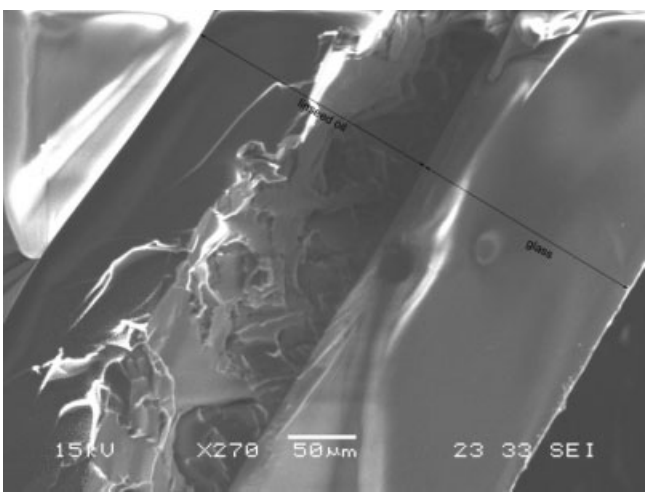

Figure 8 SEM morphology of cured linseed oil film showing a brittle layer and a gel layer. Sample was cured on a glass slide for 10 h under infrared light.

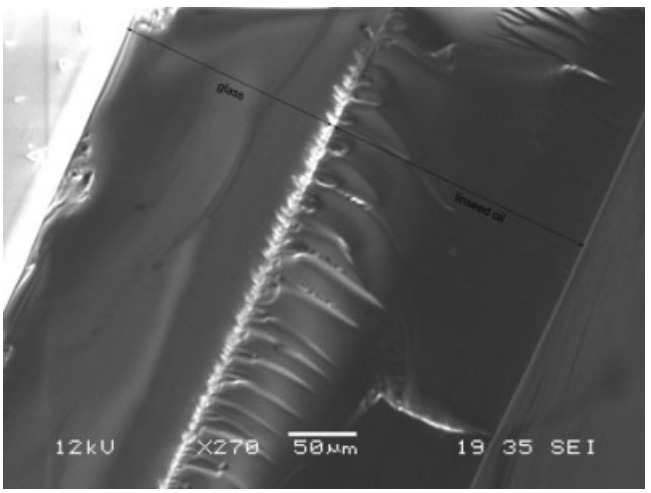

Figure 9 SEM morphology of cured linseed oil film showing a brittle layer and a ductile layer. Sample was pretreated with gamma radiation at 25 kGy and cured on a glass slide for 10 h under infrared light.

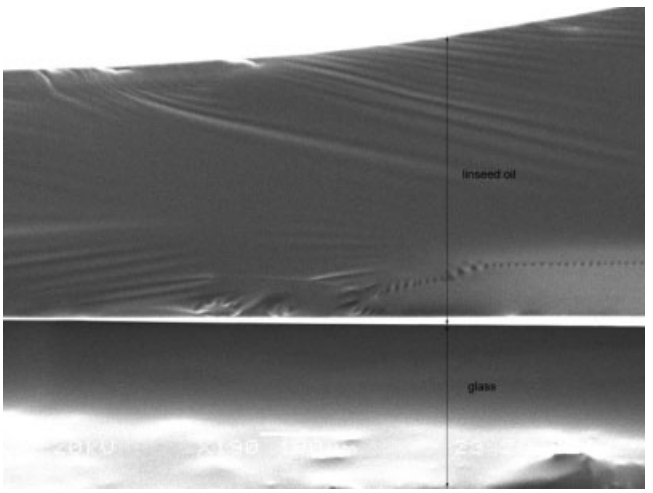

Figure 10 SEM morphology of a cured linseed oil film showing a soft gel layer. Sample was pretreated with gamma radiation at 50 kGy and cured on a glass slide for 8 h.

Very smooth surfaces with parallel lines were typical of brittle fracture, whereas rough surfaces with more threads were found in ductile failures. In another report, He et al.[29] investigated the tensile fracture of $(Fe_{0.5}Ni_{0.5})_{80-x}Mo_xB_{20}$ (x = 0–8) amorphous alloys. They reported that vein patterns corresponded with ductile materials, whereas cleavage patterns were associated with poor ductility. Eizadjou et al.[30] studied the structure and mechanical properties of multilayered Al/Au composites. SEM images after tensile tests showed dimples and shear zones which were associated with ductile failures. Gamez-Perez et al.[31] studied the fracture behavior of ethylene propylene block copolymers. They reported that the fracture surface of ductile materials was irregular whereas the texture of brittle samples was uniform. Similar texture patterns in SEM images were observed in biodegradable blends of poly(L-lactide), poly(ethylene succinate)[32] and in polypropylene/poly(styrene-ran-butadiene) blends.[33]

The bottom layer in Figure 8 shows a spongy structure formed by thin films and fibers apparently entrapping liquid oil. In Figure 9, the surface appears glassy, consistent with hard and brittle materials. Figures 8 and 9 suggested a stage wise curing process, where irradiation may have contributed to increase curing rates. Based on SEM images, a qualitative model for film curing was proposed. A skin was first formed on the oil surface, where abundant oxygen was available for oxidative polymerization processes. The skin hardened by continued polymerization until a hard layer was formed. Underneath this layer, oxygen supply was limited because of impaired diffusion by the dense top layer and polymerization went at a slower rate. As the process continued, oil changed from liquid to gel and then to a ductile solid, ultimately forming a hard and brittle film.

Figures 10–12 show images of linseed oil films, where oil was pretreated at 50 kGy and films were dried in air for 8, 10, and 14 h, respectively. Images show three stages in the drying of linseed oil. Figure 10 shows only one layer containing a uniform pattern resulting from a high plastic deformation. It was associated with a gel-like fracture. Images in Figures 11 and 12 show two layers, a top hard layer and a gel-like bottom layer. The top layer thickness increased with curing time, from 10% of the total thickness in Figure 11 to 30% in Figure 12. The drying of linseed oil was thought to take place in stages. First, the top layer changed from liquid to gel. This

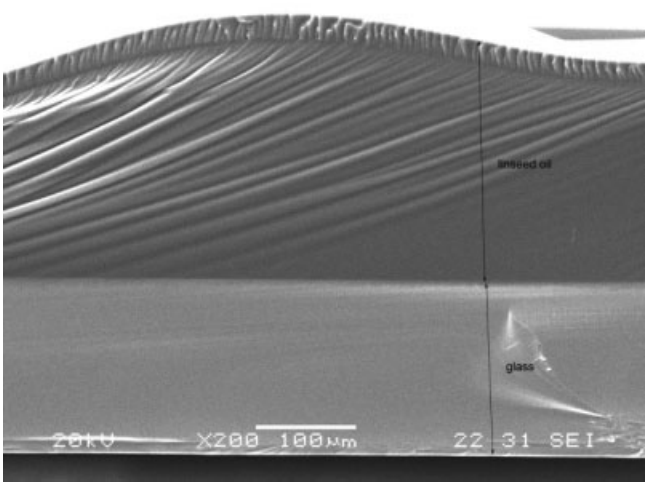

Figure 11 SEM morphology of cured linseed oil film showing brittle and gel layers. Sample was pretreated with gamma radiation at 50 kGy and cured on a glass slide for 10 h.

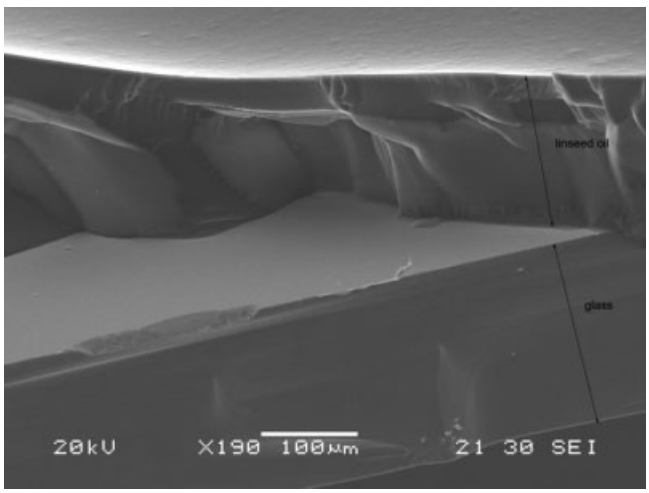

Figure 12 SEM morphology of a cured linseed oil film showing a brittle layer. Sample was pretreated with gamma radiation at 50 kGy and cured on a glass slide for 14 h.

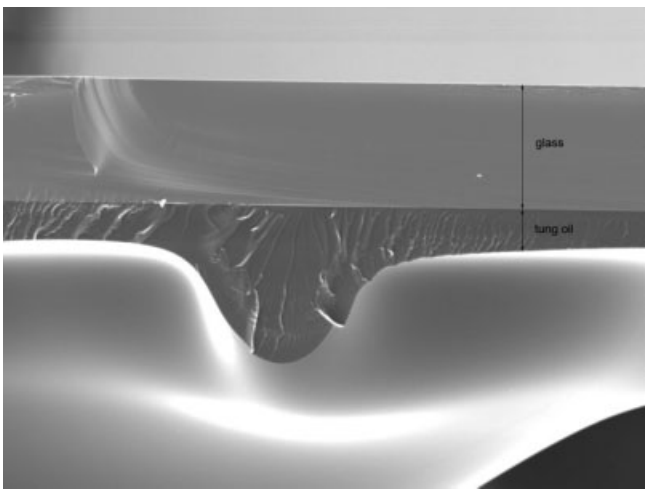

Figure 14 SEM morphology of a drying tung oil film showing shrinking of the skin layer. Sample was pretreated with gamma radiation at 25 kGy and cured on a glass slide for 6 h under infrared light.

top layer hardened by oxidation/polymerization because oxygen was available from air. The bottom layer lagged behind in its transformation from liquid to gel, then to ductile solid, and ultimately to brittle solid. Oxygen diffusion through the bottom layers was impaired by the hardened top layer and oxygen concentration decreased with depth. With increasing drying time, the top layer became thicker, until the whole of the cross section became hard and brittle.

SEM images in Figures 13–15 show the morphology of tung oil films cured on glass slides. Samples were dried under infrared light for 6 h. Images were taken from the freeze-fracture surface of films. SEM images suggested a different model for the curing of tung oil from that proposed for linseed oil. In contact with air, tung oil appeared to form thin skins very quickly. The skins hardened through oxidative polymerization and became compact and dense.[28] Shrinkage of the skin layer allowed exposure of the liquid oil underneath, which hardened in turn upon contact with air. Continuous formation of new skin warped the film surface (Fig. 14), which became separated from the glass slide support (Fig. 15).

Previous research in our lab on the application of drying oils as coatings for protein films suggested that films coated with linseed or tung oils developed different mechanical properties (results not published). Tung oil coatings were brittle and prone to develop cracks upon film stretching. Linseed oil coatings showed higher elongation than tung oil coatings, possibly because of the presence of a

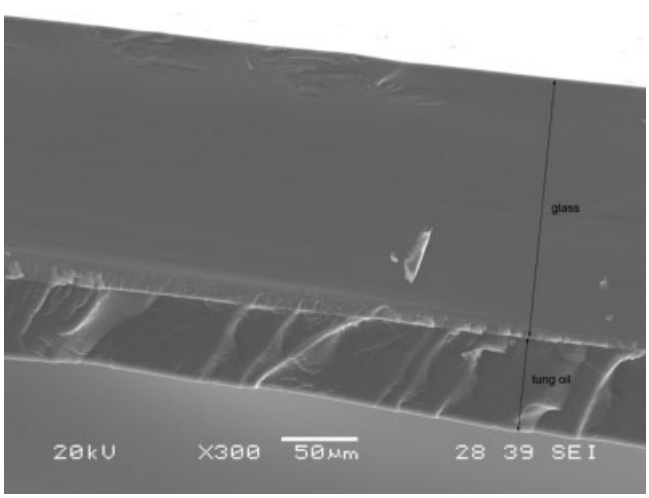

Figure 13 SEM morphology of cured tung oil film showing a thin brittle layer. Sample was cured on a glass slide for 6 h under infrared light.

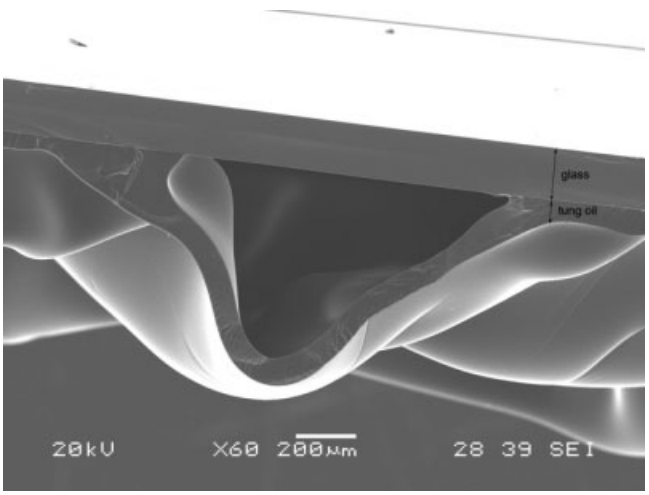

Figure 15 SEM morphology of a drying tung oil film showing warping of the skin layer. Sample was pretreated with gamma radiation at 50 kGy and cured on a glass slide for 6 h under infrared light.

ductile bottom layer. Under the same conditions, tung oil was considered to dry faster than linseed oil. This was possibly because of faster oxygen diffusion in tung oil than in linseed oil. As explained earlier, cracks on the skin layer of tung oil during drying allowed faster oxygen diffusion, whereas the solid top layer of linseed oil slowed down the rate of oxygen permeation.

CONCLUSIONS

FTIR was useful to monitor oil drying by measuring the decrease in absorbance at 3010 cm^{-1}, attributed to *cis* =C—H bonds. Infrared radiation was found to increase the drying rate of linseed and tung oils. Oil pretreatment with gamma radiation also increased the drying rate of both oils. Differences in morphology between linseed oil and tung oil films were observed by SEM. Linseed oil film structure typically showed two layers, a brittle top layer and a ductile bottom layer. Layered structures were believed as the result of limited oxygen availability for oxidation and polymerization reactions at the bottom layers. In contrast, the structure of tung oil films consisted of a thin brittle layer of large surface area. Film structure may affect industrial applications of drying oils. Linseed oil films may be expected to be ductile and resist cracks whereas tung oil coatings may be expected to be hard and brittle.

The authors wish to thank Phillip H. Geil for his suggestions in the preparation of this manuscript.

References

1. Davis, G.; Song, J. H. Ind Crop Prod 2006, 23, 147.
2. Wang, Q.; Padua, G. W. J. Agric Food Sci 2005, 53, 3444.
3. Mallegol, J.; Lemaire, J.; Gardette, J.-L. Prog Org Coat 2000, 39, 107.
4. Ballard, R. L.; Williams, J. P.; Njus, J. M.; Kiland, B. R.; Soucek, M. D. Eur Polym J 2001, 37, 381.
5. Stenberg, C.; Svensson, M.; Wallstorm, E.; Johansson, M. Surf Coat Int B: Coat Trans 2005, 88, 119.
6. Booth, G.; Delatte, D. E.; Thams, S. F. Ind Crop Prod 2007, 25, 257.
7. Odlyha, M. Thermochim Acta 1995, 269, 705.
8. Lazzari, M.; Chiantore, O. Polym Degrad Stab 1999, 65, 303.
9. Hutchinson, G. H. J. Oil Colour Chem Assoc 1973, 56, 303.
10. Bat, E.; Gunduz, G.; Kisakurek, D.; Akhmedov, I. M. Prog Org Coat 2006, 55, 330.
11. Mills, J. S.; White, R. In The Organica Chemistry of Museum Objects;Mills, J. S., White, R., Eds.; Butterworth and Heinemann: Oxford, U.K., 1994; p 31.
12. Wang, Y.; Wang, Q.; Artz, W. E.; Padua, G. W. J. Agric Food Chem 2008, 56, 3043.
13. Wicks, Z. W.; Jones, F. N.; Pappas, S. P. Organic Coatings Science and Technology; Wiley/ VCH: Weinheim, Germany, 1999; p 39.
14. Gryglewicz, S.; Grabas, K.; Gryglewicz, G. Bioresour Technol 2000, 75, 213.
15. Boyatzis, S.; Ioakimoglou, E.; Argitis, P. J. Appl Polym Sci 2002, 84, 936.
16. Coffey, S. J. Chem Soc 1922, 121, 17.
17. Ioakimoglou, E.; Boyatzis, S.; Argitis, P.; Fostiridou, A.; Papapanagiotou, K.; Yannovits, N. Chem Mater 1999, 11, 2013.
18. Van Gorkum, R.; Bouwman, E. Coord Chem Rev 2005, 249, 1709.
19. Van Der Weerd, J.; Van Loon, A.; Boon, J. J. Stud Conservat 2005, 50, 3.
20. Mosiewicki, M. A.; Rojas, O.; Sibaja, M. R.; Borrajo, J.; Aranguren, M. I. Polym Int 2007, 56, 875.
21. Rhim, J. W.; Gennadio, A.; Fu, D.; Weller, C. L.; Hanna, M. A. Food Sci Technol Lebensm Wiss Technol 1999, 32, 129.
22. Urbain, W. M. In Radiation Chemistry of Major Food Components; Elias, P. S., Cohen, A. J., Eds.; Elsevier Scientific Publishing: Amsterdam, The Netherlands, 1977; p 63.
23. Cheftel, J. C.; Cuq, J. L.; Lorient, D. In Food Chemistry; Fennema, O. R., Ed.; Dekker: New York, 1985; p 245.
24. Ahmad, S.; Ashraf, S. M.; Zafar, F. J. Appl Polym Sci 2007, 104, 1143.
25. Vlachos, N.; Skopelitis, Y.; Psaroudaki, M.; Konstantinidou, V.; Chatzilazarou, A.; Tegou, E. Anal Chim Acta 2006, 573, 465.
26. Polovka, M.; Brezova, V.; Stasko, A.; Mazur, M.; Suhaj, M.; Simko, P. Radiat Phys Chem 2006, 75, 309.
27. Guillen, M. D.; Ruiz, A.; Cabo, N.; Chirinos, R.; Pascual, G. J. Am Oil Chem Soc 2003, 80, 755.
28. Lin, Y.; Zhang, K.-Y.; Dong, Z.-M.; Dong, L.-S.; Li, Y.-S. Macromolecules 2007, 40, 6257.
29. He, Z. Q.; Wang, X. L.; Zhao, Z. Y.; Quan, B. Y. J Non-Cryst Solids 2008, 354, 1683.
30. Eizadjou, M.; Talachi, A. K.; Manesh, H. D.; Shahabi, H. S.; Janghorban, K. Compos Sci Tech 2008, 68, 2003.
31. Gamez-Perez, J.; Munoz, P.; Santana, O. O.; Gordillo, A.; Maspoch, M. L. J. Appl Polym Sci 2006, 101, 2714.
32. Lu, J.; Qiu, Z.; Yang, W. Polymer 2007, 48, 4196.
33. Hristov, V.; Lach, R.; Krumova, M.; Grellmann, W. Polym Int 2005, 54, 1632.